Supporting Information

Bilayer SnO_2 as Electron Transport Layer for Highly Efficient Perovskite Solar Cells

Haimang Yi[*,†], *Dian Wang*[†], *Md Arafat Mahmud*[†], *Faiazul Haque*[†], *Mushfika Baishakhi Upama* [†], *Cheng Xu*[†], *Leiping Duan*[†] *and Ashraf Uddin*[*,†]

AUTHOR ADDRESS

[†]School of Photovoltaic and Renewable Energy Engineering, University of New South Wales, Sydney, NSW 2052, Australia

Corresponding Author

*E-mail: haimang.yi@student.unsw.edu.au. (H.Y.)

*E-mail: a.uddin@unsw.edu.au. (A.U.)

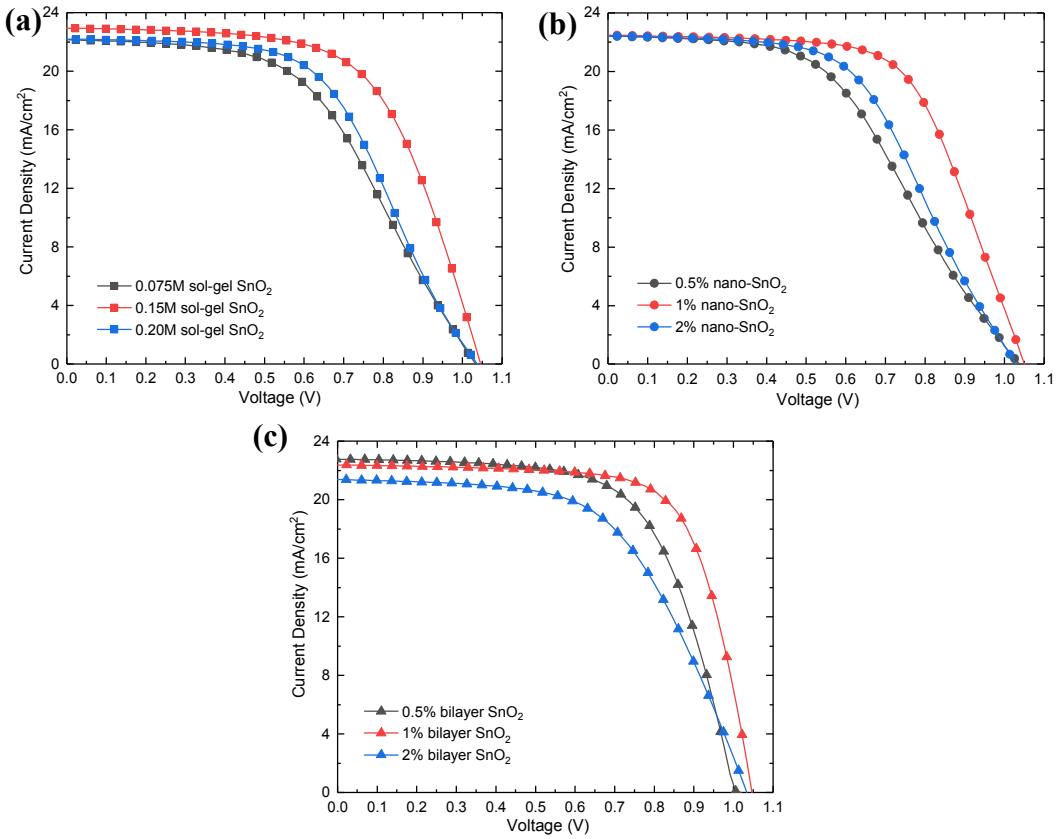

Fig. S1 J-V curves of (a) sol-gel SnO_2, (b) nano-SnO_2 and (c) bilayer SnO_2 with different concentration

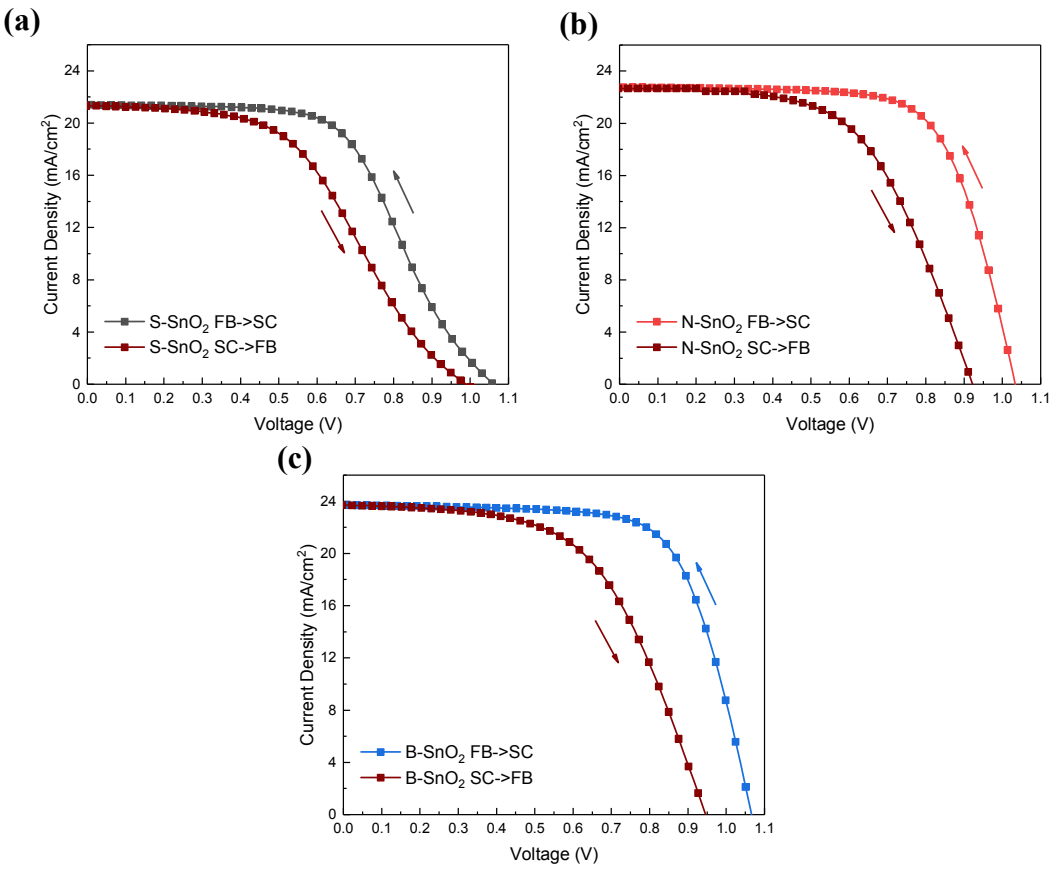

Fig. S2 J-V curves (both FB-SC and SC-FB direction at 0.05 V/s) of the (a) S-SnO_2, (b)N-SnO_2 and (c)B-SnO_2 device.

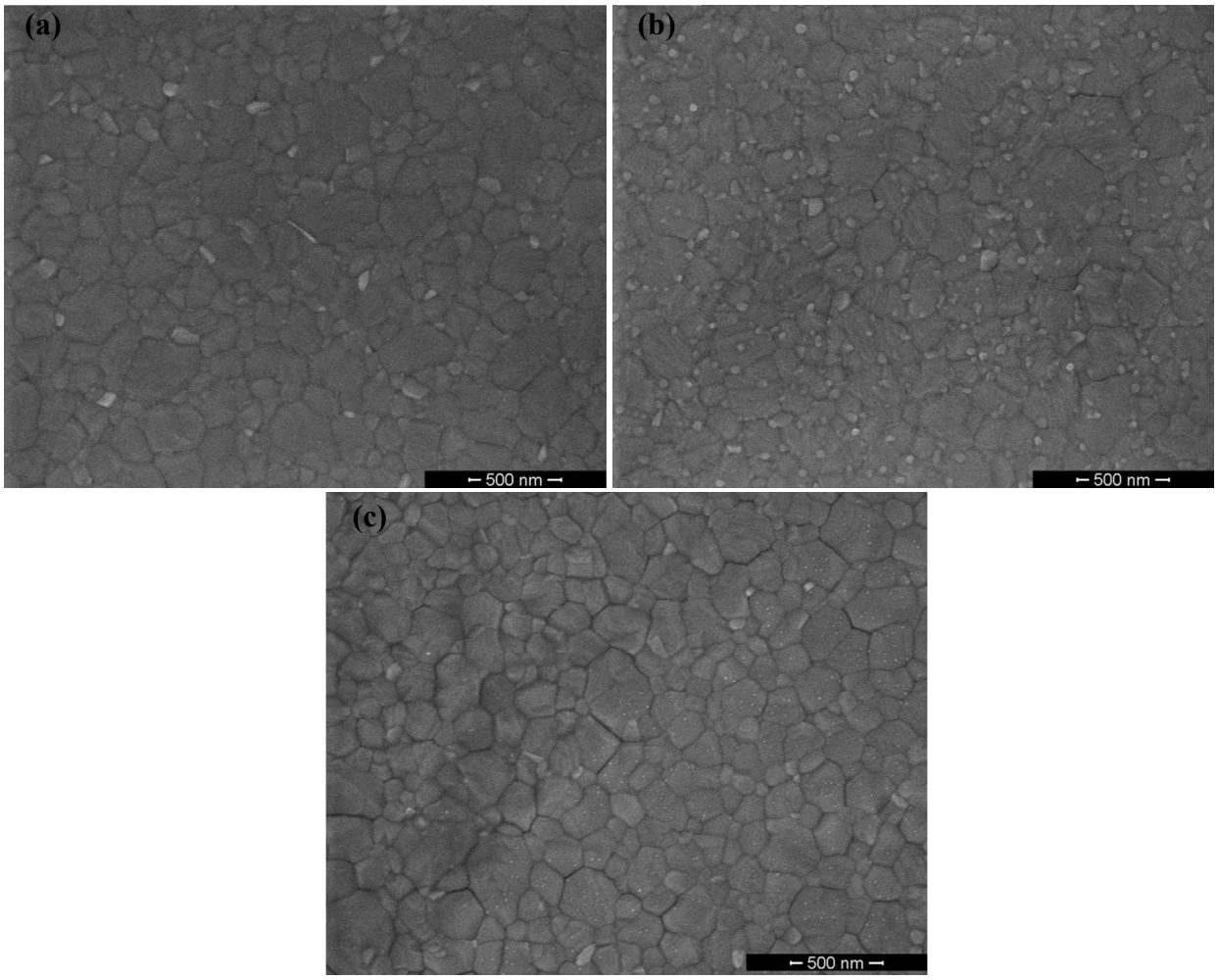

Fig. S3 Top view Scanning Electron Microscopy (SEM) images of $MAPbI_3$ perovskites deposited on (a) S-SnO_2; (b) N-SnO_2 and (c) B-SnO_2 films

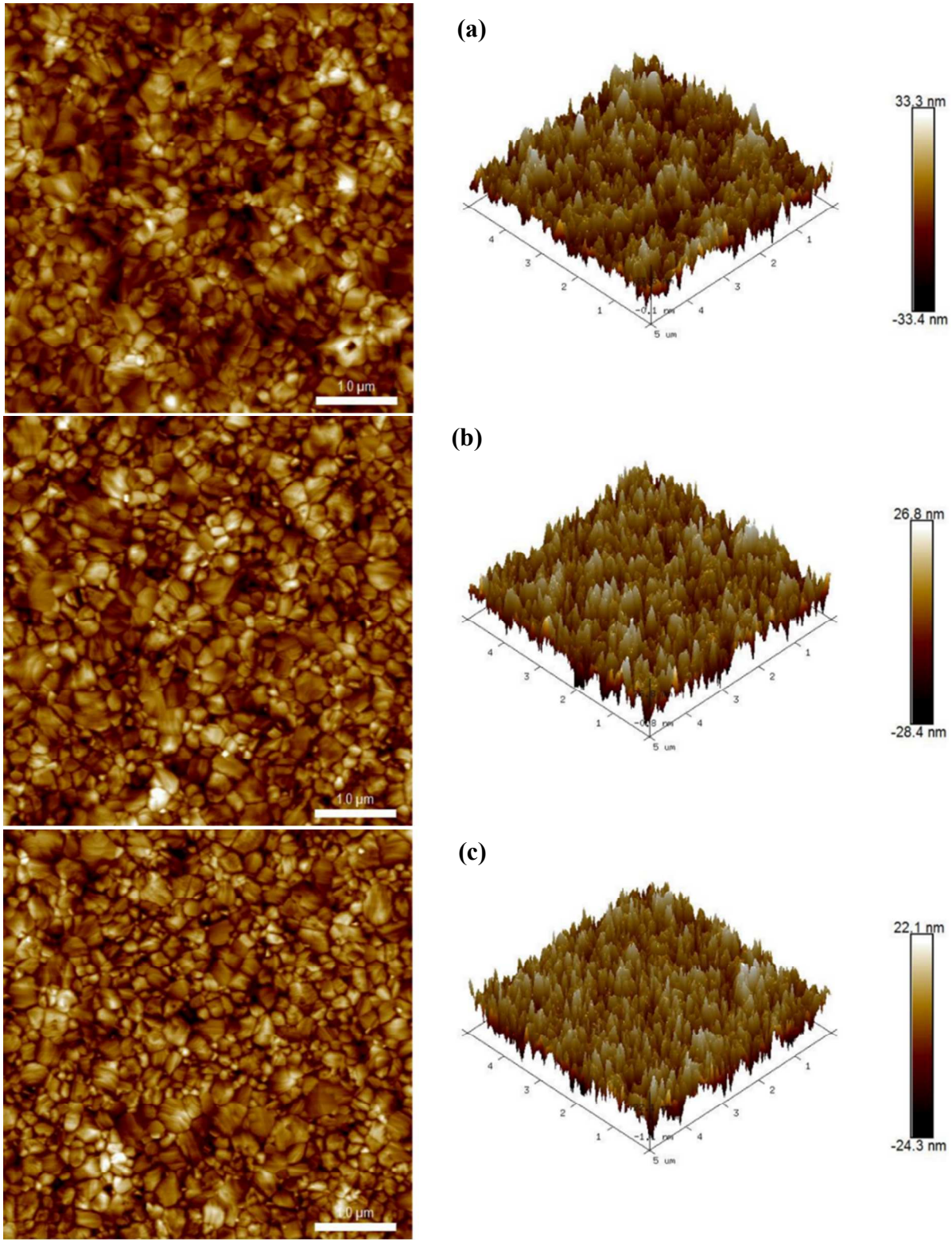

Fig. S4 Two and three-dimensional atomic force microscopy (AFM) images of $MAPbI_3$ perovskites deposited on (a) S-SnO_2; (b) N-SnO_2 and (c) B-SnO_2 films

Table S1

Device performance parameters of perovskite devices with different thickness of sol-gel SnO_2, nano-SnO_2 and bilayer SnO_2 ETLs, under one sun illumination (AM 1.5G, 100mW·cm^{-2}).

	V_{oc} (V)	J_{sc} (mA/cm^2)	FF (%)	PCE (%)
0.075M sol-gel	0.95 ± 0.096	21.33 ± 0.85	49.76 ± 7.14	10.03 ± 1.31
0.15M sol-gel	1.03 ± 0.029	21.81 ± 0.68	57.60 ± 4.50	12.97 ± 1.16
0.20M sol-gel	1.00 ± 0.033	21.87 ± 0.56	45.55 ± 5.94	10.04 ± 1.63
0.5% Nano	0.73 ± 0.081	19.32 ± 0.79	64.11 ± 2.69	9.06 ± 1.36
1% Nano	1.03 ± 0.035	22.24 ± 0.67	61.44 ± 1.57	14.05 ± 1.08
2% Nano	1.02 ± 0.039	21.99 ± 1.06	56.53 ± 5.96	12.62 ± 0.90
0.15M+0.5%	1.01 ± 0.021	22.08 ± 0.45	60.86 ± 2.08	13.58 ± 0.50
0.15M+1%	1.05 ± 0.017	22.49 ± 0.89	71.25 ± 1.41	16.84 ± 0.53
0.15M+2%	1.01 ± 0.051	21.10 ± 0.34	55.48 ± 1.78	11.85 ± 1.01

Table S2

Start, peak and end binding energy of elemental peaks, peak width/full width at half maximum and atomic percentage of ETL films (S-SnO_2, N-SnO_2 and B-SnO_2) calculated by the spectral fitting from X-Ray photoelectron spectroscopy (XPS) data.

ETL	Peak	Start Binding Energy (eV)	Peak Binding Energy (eV)	End Binding Energy (eV)	Full Width at Half Maximum (FWHM) (eV)	Atomic Percentage (%)
S-SnO_2	$O_{1s\ A}$	534.72	532.14	527.12	1.66	37.3
	$O_{1s\ B}$	534.72	530.49	527.12	1.66	38.21
N-SnO_2	$O_{1s\ A}$	535.04	532.36	527.44	1.54	21.87
	$O_{1s\ B}$	535.04	530.6	527.44	1.54	47.29
B-SnO_2	$O_{1s\ A}$	535.35	531.95	527.75	1.48	15.42
	$O_{1s\ B}$	535.35	530.48	527.75	1.48	50.95

Table S3

The profile surface roughness paramaeters of $MAPbI_3$ perovskite on sol-gel SnO_2, nano-SnO_2 and bilayer SnO_2 films calculated from surface topography imaging with AFM. Ra represents arithmetical mean deviation of the assessed profile, while Rq represents root mean squared value.

	R_a	**R_q (RMS)**
Perovskite on S-SnO_2	7.45 nm	9.39 nm
Perovskite on N-SnO_2	6.22 nm	7.84 nm
Perovskite on B-SnO_2	5.12 nm	6.50 nm

Table S4

Numerical Data of peak intensity, FWHM (full width half maximum), cystallite size, microstrain and dislocation density in X-ray Diffraction analysis of $MAPbI_3$ perovskite layer on different ETLs (sol-gel, nano and bilayer SnO_2)

Characteristic Peak	**ETL**	**Relative Peak Intensity**	**FWHM (Degree)**	**Crystallite Size (nm)**	**Microstrain ($*10^{-3}$)**	**Dislocation Density ($*10^{11}$ cm-3)**
(110)	S-SnO_2	8414	0.16	50.78	5.82	0.35
	N-SnO_2	9256	0.15	54.61	5.41	0.37
	B-SnO_2	9170	0.15	55.95	5.28	0.35
(220)	S-SnO_2	3927	0.17	49.45	2.98	0.46
	N-SnO_2	3738	0.18	48.01	3.07	0.47
	B-SnO_2	3842	0.18	48.88	3.02	0.46
(310)	S-SnO_2	2171	0.20	43.78	3.02	0.69
	N-SnO_2	2338	0.20	43.14	3.06	0.59
	B-SnO_2	2205	0.22	39.81	3.31	0.69
(224)	S-SnO_2	629	0.25	35.07	2.97	1.07
	N-SnO_2	694	0.23	38.86	2.68	0.72
	B-SnO_2	653	0.28	31.90	3.27	1.07
(314)	S-SnO_2	428	0.33	26.98	3.65	1.47
	N-SnO_2	440	0.35	25.87	3.80	1.63
	B-SnO_2	448	0.33	27.21	3.62	1.47